Article

A Comparative Study of Electrochemical and Optical Properties of Rhenium Deposited on Gold and Platinum

Jorge O. Zerbino[a], Ana M. Castro Luna[a], Carlos F. Zinola[b], Eduardo Méndez[b] and M. E. Martins[,a]*

[a]INIFTA, Universidad Nacional de La Plata, Sucursal 4, C.C. 16 (CP 1900), La Plata, Argentina

[b]Laboratorio de Electroquímica Fundamental, Facultad de Ciencias, Iguá 4225, Universidad de la República, Montevideo, CP 11400, Uruguay

Filmes de rênio e de óxido de rênio foram depositados sobre eletrodos de ouro e platina aplicando polarizações potenciostáticas e potenciodinâmicas numa região compreendida entre – 0,20 V e 0,70 V (*vs rhe*) em meio aquoso ácido contendo íons perrenato. As espessuras e as variáveis óticas dos filmes foram obtidas empregando perturbações triangulares de potencial e técnicas elipsométricas. Sobre eletrodos de ouro foi depositado rênio metálico na região de potencial de formação de hidrogênio molecular. Sobre eletrodos de platina foi formado óxido de rênio na região de adsorção de átomos de hidrogênio e rênio metálico juntamente com a formação de hidrogênio adsorvido e molecular sobre o mesmo metal.

Rhenium-containing films were grown on gold and platinum after different potentiostatic and potentiodynamic polarizations in the - 0.20 V to 0.70 V range (*vs rhe*) in aqueous acid perrhenate. Experimental data were obtained using cyclic voltammetry and ellipsometry, from which the thickness and optical indices of the electrodeposited rhenium layer were calculated. Metallic rhenium deposition on gold takes place at potentials within the hydrogen evolution reaction. Rhenium oxide on platinum is formed in the hydrogen adatom potential domain, whereas metallic rhenium is deposited concurrently with the hydrogen adsorption and evolution reactions on the same metal.

Keywords: rhenium, gold, platinum, voltammetry, ellipsometry

Introduction

The electrochemistry of rhenium has been the subject of different studies because of its catalytic properties in fuel cell electrodes and as a coordination compound in radiopharmacy.[1-3] The electrodeposition of rhenium species on gold from aqueous perrhenate solutions has been investigated by Horanyi *et al.*,[4] concluding that metallic rhenium is deposited at potentials within the hydrogen evolution region. By using an electrochemical quartz microbalance,[5] it has been found that rhenium deposition occurs through a mechanism of progressive nucleation, which changes from two-dimensional to three-dimensional growth, under diffusion control. However, the nature of the adsorbed layer has not been yet identified.[5] On platinum, on the other hand, some kind of oxygen-containing rhenium species has been detected, probably

ReO$_2$.[6] It has been suggested that prior to hydrogen electroadsorption ReO$_2$ adsorption takes place, and after the layer completion, bulk phases of ReO$_2$ and ReO$_3$ can be also observed.[7]

In the present work additional information obtained by spectroscopic *in situ* ellipsometry may contribute to solve the controversy still existing about the nature of the electrodeposited layer both on platinum and on gold.

Experimental

The electrochemical and ellipsometric studies were performed using a three-electrode optical cell as previously reported.[8] Polycrystalline (*pc*) gold and platinum disks (0.95 and 1.05 cm^2 real area) were used as working electrodes, which were mirror polished with fine grade alumina powders (0.3 and 0.05 mm). A large gold or platinum gauze was used as counter electrode and a reversible hydrogen electrode (*rhe*) as reference.

Aqueous 1 mol L^{-1} H$_2$SO$_4$ (T. J. Baker, ACS reagent) and

10^{-3} mol L^{-1} aqueous NH_4ReO_4 (Aldrich, 99 + %) in 1 mol L^{-1} H_2SO_4 were used as supporting electrolyte and working solution, respectively. Solutions were prepared from analytical quality chemicals reagent and Millipore-Milli-Q* water. All runs were performed under oxygen-free nitrogen gas saturation, at 298 K. Potentials in the text are given on the reversible hydrogen electrode (rhe) scale.

Cyclic voltammetry was performed with pc gold or platinum electrodes in the supporting electrolyte and in the working solution at a potential scan rate $(v) = 0.1$ V s^{-1}. Voltammetric runs included repetitive triangular potential scans and potential holdings in the - 0.20 V to 0.40 V range for a fixed time τ.

Ellipsometry was performed illuminating the electrode with monochromatic light in the visible wavelength range (400 nm $\leq l \leq$ 700 nm) with an incident angle of 70 degrees. The ellipsometric parameters Δ and ψ were measured at different λ, i.e. 405, 450, 492, 546 and 580 nm.

Different experimental procedures were applied for electrochemical and ellipsometric measurements depending on the nature of the electrode surface.

Gold electrodes

Procedure A. The electrode potential was held in the - 0.20 V $\leq E_c \leq$ 0.20 V range for a time τ. Later, a second potential holding at E_c = 0.10 V was applied for τ = 10 min under nitrogen bubbling, allowing the electrooxidation of molecular hydrogen previously formed. Finally, repetitive triangular potential scans were applied from E_c = 0.10 V to E_a = 1.70 V.

Procedure B. First, a potential holding at E_a = 1.20 V for τ = 3 min was adjusted in the cell. Then, a potential scan at a sweep rate $v = 5 \times 10^{-4}$ V s^{-1} from E_a to a cathodic potential E located within the - 0.20 V $\leq E \leq$ 0.20 V range was applied. After reaching E and holding the potential for τ = 10 min, an upscan from E to E_a was subsequently performed. Ellipsometric parameters Δ and ψ were recorded when applying the potential routine, as a function of potential E and time t.

Platinum electrodes

Procedure C. Ellipsometric parameters Δ and ψ were recorded as a function of the potential E at $v = 5 \times 10^{-4}$ V s^{-1} from E_a = 0.70 V to E_c = 0.03 V and subsequently an upscan was applied from E_c to E_a.

Procedure D. The electrode potential was held in the 0.03V $\leq E \leq$ 0.15V range for a time τ = 10 min. The ellipsometric parameters Δ and ψ were recorded at the five wavelenghts and at different selected potentials.

Results and Discussion

### Electrochemical and optical behaviour of rhenium species on gold

Cyclic voltammograms of pc gold in the working solution run at v = 0.10 Vs^{-1} after holding the potential at E = - 0.15 V and subsequently at E = 0.10 V for τ = 3 and 10 min are shown in Figure 1 (Procedure A). The first increasing potential scan covering a potential domain from 0.15 V to 1.70 V, exhibits a complex anodic profile, where two current peaks at 0.75 V and 0.88 V are observed. The current contribution at $E > 1.30$ V corresponds to the oxygen electrosorption. The second and the following cyclic potential scans run up to 1.70 V reveal that the anodic contributions within the 0.15 V to 1.20 V range, which are ascribed to adsorbed rhenium species, are no longer observed.
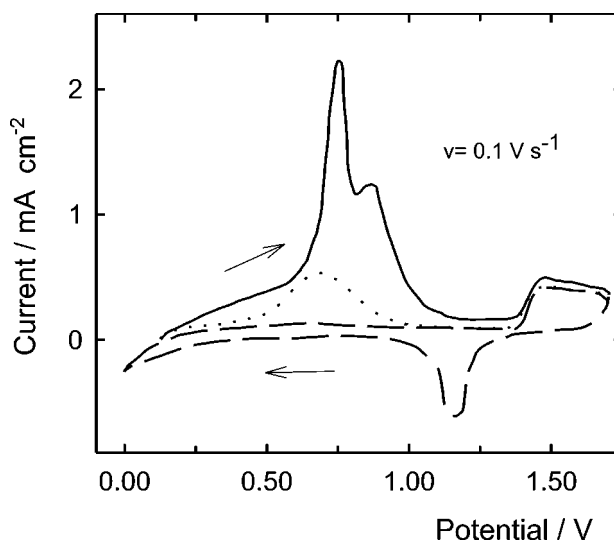
Figure 1. Cyclic voltammogram of pc gold in aqueous 10^{-3} mol L^{-1} ReO_4^- + 1 mol L^{-1} H_2SO_4 after holding the potential at E_c = - 0.15 V and subsequently at E = 0.10 V for τ = 3 min (.........) and for τ = 10 min (——). The second potential scan is denoted as (- - - -). v = 0.10 V s^{-1}. T = 298 K.

The evolution of the ellipsometric parameters Δ and Ψ, obtained applying a decreasing potential scan from E_a = 1.20 V to a cathodic potential limit E_c = - 0.20 V, is shown in Figures 2a an 2c, respectively (Procedure B). The Δ and Ψ values remain nearly constant throughout the decreasing potential scan (Figure 2a). Moreover, when E_c is applied Δ remains stable for times $\tau <$ 3 min, while for longer τ, Δ continuously decreases (Figure 2b). Afterwards, during the following positive going potential sweep, Δ still decreases until achieving a constant Δ value within the region 0.10 V $\leq E \leq$ 0.60 V. Finally, for $E >$ 0.60 V, Δ

increases reaching the initial Δ and Ψ values (Figures 2a and 2c). At $E = -0.20$ V, Δ exhibits a decrease equal to 8.7 degrees while during the upscan Ψ remains almost constant (Figures 2c and 2d). The Δ behaviour indicates that rhenium-containing species are totally desorbed from the surface during the subsequent upscan.
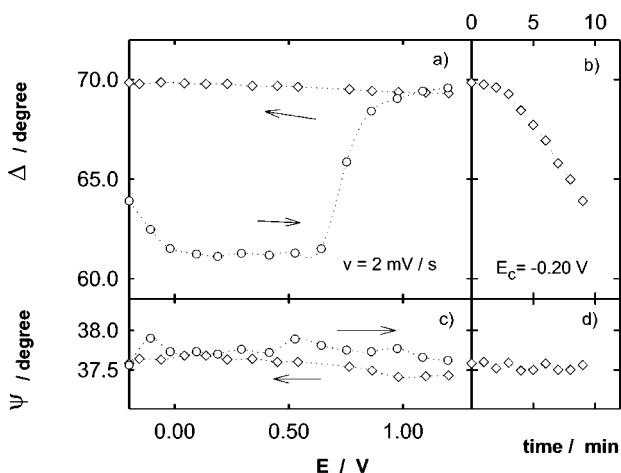

Figure 2. Evolution of ellipsometric parameters Δ and Ψ for the following sequence: (a,c) down scan from $E_a = 1.2$ V to $E_c = -0.20$ V ($\Diamond$), $v = 2$ 10^{-3} Vs^{-1}; (b,d) a potential holding for $t = 10$ min at $E_c = -0.20$ V ($\blacklozenge$); (a,c) upscan from $E_c = -0.20$ V to $E_a = 1.2$ V (o), $v = 2$ 10^{-3} V s^{-1}. Gold in aqueous 10^{-3} mol L^{-1} ReO$_4^-$ + 1 mol L^{-1} H$_2$SO$_4$. $\lambda = 546$ nm. T $= 298$ K.

The comparison between ellipsometric results and theoretical calculations considering the growth of an isotropic and homogeneous[8] layer allows a quantitative description of the electrodeposition process. For these interfaces the decrease in Δ (Ψ remaining nearly constant) may be considered as a measure of the increase in the layer thickness, d.

Optical indices $(n - i\ k)$ and the d values of the grown layer are evaluated using Δ/Ψ pairs of data measured at five λ_j. This set of optical data allows the unequivocal determination of d, n (refractive index) and k (light absorption coefficient). Furthermore, optical indices are calculated assuming the formation of a single homogeneous film of constant composition and different thicknesses according to literature.[8] The program employed for calculations uses the subroutine *IBM-DFMCG*[9] that finds the local minimum of a complex function of several variables by the conjugated gradients method. For each λ_j the experimental values corresponding to five film thicknesses d_i were fitted for a single pair of optical indices n_i and k_i. Simultaneously, for each value of d_j, the optical data measured at different λ_i must fit the same d_j value.

The calculated values of thickness d are plotted as a function of E_c (Figure 3). There is a general agreement that a metallic rhenium electrodeposit is obtained by applying
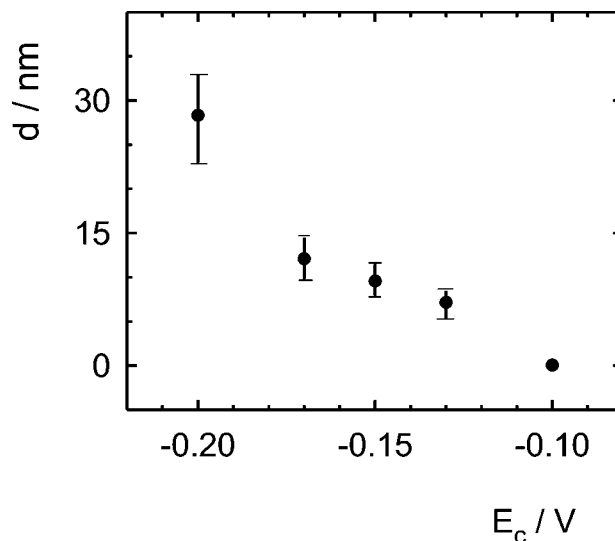

Figure 3. Thickness d of the adsorbed layer *vs* E_c calculated from ellipsometric data.

relatively high cathodic currents whereas rhenium oxide layers are possibly formed under milder reduction conditions.[6]

The optical indices of rhenium oxide have been reported[10] resulting k values in the range $0.3 \leq k \leq 0.5$ for λ within 400 nm $\leq \lambda \leq 546$ nm. Taking into account that these k values are lower than those experimentally obtained for the same λ region, $0.4 \leq k \leq 0.9$, the possibility of rhenium oxide layer formation on gold is excluded. Besides, this result suggests the growth of a porous metal layer or a composite metal/electrolyte layer which may have higher absorption k indices. Therefore, n and k values are compared with those obtained through the Bruggeman Effective Medium Theory (*EMT*) for an ideal mixture of metallic rhenium and water or metallic rhenium and hydrogen as a function of the volumetric fraction Q (metal/electrolyte, metal/vacuum).[11] These calculations are shown in Figure 4 where it is assumed: *i)* the formation of a composite of rhenium and water, and *ii)* the formation of a composite of metallic rhenium and residual molecular hydrogen gas trapped in the grown layer on *pc* gold. On the other hand, the values of effective optical indices predicted by the Maxwell Garnet Theory (*MGT*) for either metallic grains dispersed in a hydrogen matrix or voids filled with molecular hydrogen embedded in a metallic matrix were also calculated[12] (Table 1).

These data demonstrate a good agreement regarding the values of n and k predicted either by the *EMT* or the *MGT* considering hydrogen voids immersed in the metallic matrix. The calculated indices show a good agreement with the latter proposal resulting in a Q fraction of about 30 %. On the other hand, when metallic grains immersed
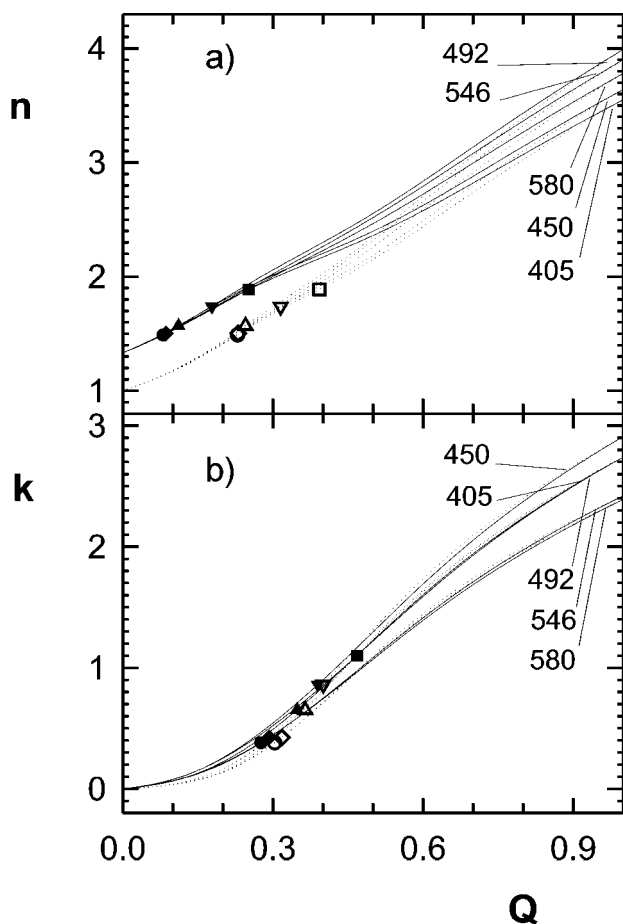
Figure 4. (a) n and (b) k values predicted by the Bruggeman Effective Medium Theory for the case of (1) the composite metallic rhenium and electrolyte vs the volumetric fraction Q, (——); λ = (●) 580 nm, (◆) 546 nm, (▲) 492 nm, (▼) 450 nm, (■) 405 nm; and for (2) the composite metallic rhenium and occluded hydrogen vs the volumetric fraction Q, (.........), λ = (○) 580 nm, (◊) 546 nm, (△) 492 nm, (▽) 450 nm, (□) 405 nm. Symbols correspond to the experimental n and k obtained after data analysis. Gold in aqueous 10^{-3} mol L^{-1} ReO$_4^{-}$ + 1 mol L^{-1} H$_2$SO$_4$. T = 298 K.

in a hydrogen matrix are taken into account, it results in a larger dispersion of the predicted Q values. This fact provides further evidence that the voids filled with hydrogen embedded in a metallic matrix suit an appropriated theory. In spite of the small differences between the predicted Q values by the EMT and the MGT for the different λ_i values, the comparison of data leads to an estimate of Q value between 20% and 30%, corresponding to a composite formed by metallic rhenium with occluded hydrogen.

Electrochemical and optical behaviour of rhenium species on platinum

Cyclic voltammograms of smooth pc platinum in the working solution run at v = 0.10 V s^{-1} from

0.05 V $\leq E_c \leq$ 0.50 V up to E_a = 1.40 V are shown in Figure 5. They exhibit a complex anodic current peak at 0.57 V (I_a) and a broad cathodic current peak extending from 0.60 V to 0.05 V (I_c). Furthermore, a total blockage of hydrogen electrodesorption and a distorted profile of oxygen electroadsorption are observed, probably due to rhenium species competing for platinum surface sites. The gradual decrease of E_c from 0.50 V to 0.05 V results in a corresponding gradual growth of the anodic charge related to peak I_a, confirming that the broad cathodic current extending from 0.05 V to 0.60 V is related to the electrodeposition of rhenium species. Hence, these species are probably responsible of the hindrance of the hydrogen electrosorption reaction, as revealed through the feeble hydrogen electrodesorption current peaks (Figure 5).
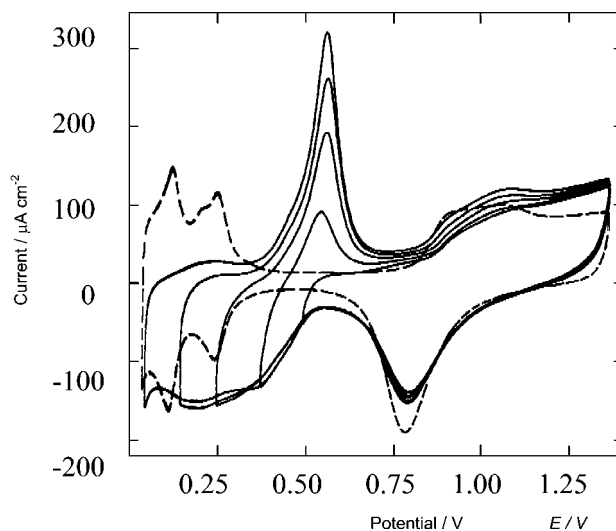
Figure 5. Cyclic voltammograms of smooth pc platinum in aqueous 10^{-3} mol L^{-1} ReO$_4^{-}$ + 1 mol L^{-1} H$_2$SO$_4$ (——) and in aqueous 1 mol L^{-1} H$_2$SO$_4$ (- - - -) with a gradual change of E_c. v = 0.10 Vs^{-1}. T= 298 K.

The evolution of Δ and Ψ during a negative going potential scan from 0.70 V to 0.03 V (Procedure C) is shown in Figure 6. In the same figure Δ and Ψ values measured at E_c = 0.20, 0.10, 0.03, 0.45 and 0.70 V, either after τ = 1 min or τ = 10 min, are also shown (Procedure D). The optical parameters in the supporting electrolyte, remain practically constant both in the double layer and hydrogen adatom potential domains (0.03 V $< E <$ 0.70 V)[15,16] and in the working solution a decrease in Δ for $E <$ 0.20 V is observed. Besides, Δ values remain constant during the early steps of the positive potential scan, but increase for $E >$ 0.25 V reaching at E = 0.70 V similar values to those observed on the freshly polished electrode. A decrease of about 0.1 degrees in Ψ is observed at 0.70 V after a potential cycle (Figure 6).
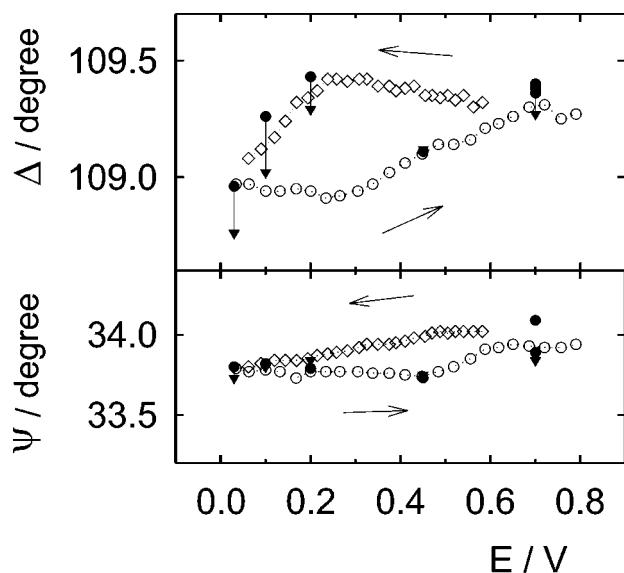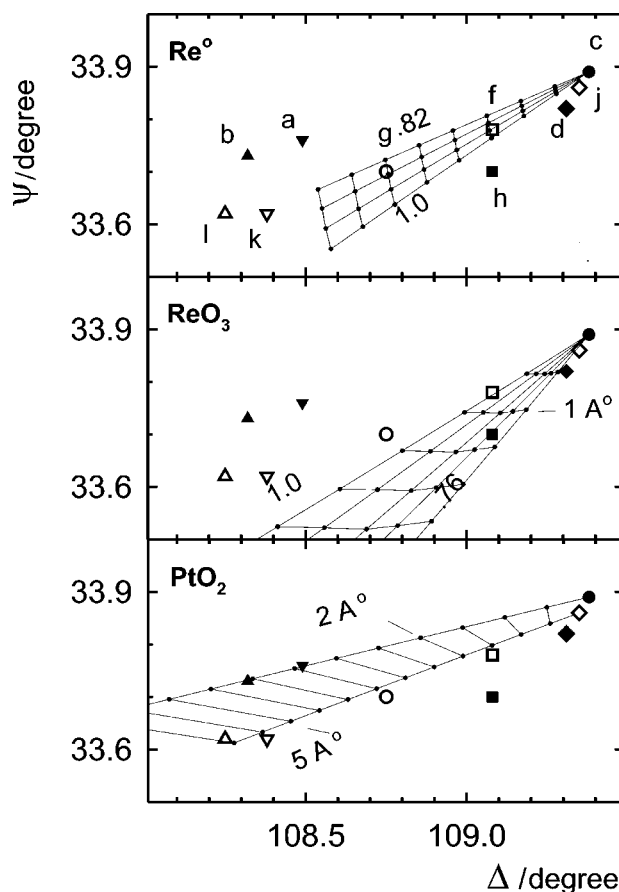
Figure 6. Evolution of ellipsometric parameters Δ and Ψ for the following sequence: (◊) down scan from $E_a = 0.70$ V to $E_c = 0.03$ V; (o) upscan from $E_c = 0.03$ V to $E_a = 0.70$ V, $v = 5 \cdot 10^{-4}$ Vs^{-1}, (Procedure C). Full marks corresponds to measurements according to Procedure D, (●) $\tau = 1$ min, (▼) $\tau = 10$ min. Platinum in aqueous 10^{-3} mol L^{-1} ReO$_4^-$ + 1 mol L^{-1} H$_2$SO$_4$. $\lambda = 546$ nm. T = 298 K.

Furthermore, Δ and Ψ values were also obtained after holding the potential at different E_c for $t = 10$ min according to Procedure D (Figure 7). The values of (d) and ($n - $ i k) of the grown layer were evaluated using Δ and Ψ data measured at the five wavelengths. Similarly to the methodology used for rhenium deposition on gold, the optical indices for platinum were calculated assuming the formation of a single homogeneous film of constant composition and different thicknesses. The program employed for the calculation also uses the subroutine *IBM-DFMCG.*[9]

In Figure 7 the calculated values of Δ and Ψ for metallic rhenium, rhenium oxide and platinum oxide layers are plotted as a function of different volume fractions, namely, Q_{ox}, oxide/ electrolyte, and Q_{met}, metal/ electrolyte, using the effective optical indices predicted by the *EMT*. Table 1 shows the optical indices and the literature value[13-16] used for the calculations. The optical indices for ReO$_2$ are similar to those of ReO$_3$ but exhibit lower k values.[10,14]

Figure 7. Δ and Ψ measured at $\lambda = 580$ nm according to Procedure D, $t = 10$ min, and the following sequence: a) (▼) $E=$ 1.4 V; b) (▲) $E=$ 1.5 V; c) (●) $E=$ 0.70 V; d) (◆) $E=$ 0.20 V; f) (□) $E=$ 0.10 V; g) (o) $E=$ 0.03 V; h) (■) $E=$ 0.45 V; j) (◊) $E=$ 0.70 V; k) (∇) $E=$ 1.4 V; l) (△) $E=$ 1.5 V. Plots include theoretical values predicted for the different layers, increasing d on each 0.5 Å: metallic rhenium, $Q = 1.00$, 0.94, 0.88, 0.82; rhenium oxide, $Q = 1.00$, 0.94, 0.88, 0.82, 0.76; platinum oxide: (▲, ▼) n - i $k = 3.38 - $ i 1.26; (∇, △) n - i $k = 2.80 - $ i 2.14.

The optical measurements agree with the formation of a layer of about 0.5 Å for ReO$_3$ ($Q_{ox} = 0.76$, $n - $ i $k=$ 0.89 − i 0.56) at $E = 0.20$ V, 3 Å for metallic rhenium ($Q_{met} = 0.88$, $n - $ i $k=$ 3.47 − i 2.13) at $E = 0.03$ V and 1.40 Å for ReO$_3$ ($Q_{ox} = 0.82$, $n - $ i $k=$ 0.85 − i 0.6) at $E = 0.45$ V. The decrease of about 0.05 degrees observed at 0.70 V probably indicates that a small quantity of rhenium oxide remains on the

Table 1. Optical indices, n and k, for metallic rhenium, rhenium oxide and platinum oxide for different values of wavelengths. $n_{water} = (1.332 - $ i 0.0), $n_{hydrogen} = (1.0 - $ i 0.0)

λ/nm	405		450		492		546		580		Ref.
	n	k	n	k	n	k	n	K	n	k	
Re	3.55	2.74	3.64	2.91	3.99	2.74	3.90	2.42	3.78	2.39	13
ReO$_3$	2.46	0.507	2.22	0.338	1.57	0.285	0.850	0.471	0.707	0.700	14
PtO$_2$	2.10	2.20	2.30	2.30	2.40	2.50	2.50	2.70	2.40	2.80	15
	3.10	1.50	3.20	1.45	3.30	1.42	3.40	1.41	3.50	1.40	16

platinum electrode after the potential cycling. Figure 7 also shows the fitting of Δ and Ψ values corresponding to PtO_2 layers at $E = 1.40$ and 1.50 V.

Conclusions

For gold electrodes rhenium deposition occurs simultaneously with hydrogen evolution reaction. A composite of metallic rhenium and occluded hydrogen is obtained with a rhenium volumetric fraction of about 30%.

For platinum electrodes, rhenium oxide grows at potentials lower than 0.20 V, whereas metallic rhenium is observed at potentials lower than 0.10 V, simultaneously with the hydrogen adatom electrosorption reaction. Multilayer growth of metallic rhenium with thickness from 50 Å to 300 Å is observed at potentials lower than - 0.10 V, while a monolayer growth of metallic rhenium occurs within the hydrogen adatom potential domain with thickness from 1.5 Å to 3.0 Å.

These results clearly indicate the strong influence of the electric potential on the behaviour of rhenium deposition. Moreover, it is also noticeable the nature of the metal electrode, taking into account that different adsorption and /or catalytic reactions are probably involved.

Acknowledgements

References

1. Karasikov, V. L.; *Elektrokhimiya* **1981**, *17*, 1518.

2. Gómez, J.; Gardiazábal, J. I.; Schrebler, R.; Gómez, H.; Córdova, R.; *J. Electroanal. Chem.* **1989**, *260*, 113.

3. Horanyi, G.; Bakos, I.; Szabó, S.; Rizmayer, E. M.; *J. Electroanal. Chem.* **1992**, *337*, 365.

4. Bakos, I.; Horanyi, G.; Szabó, S.; Rizmayer, E. M.; *J. Electroanal. Chem.* **1993**, *359*, 241.

5. Schrebler, R.; Cury, P.; Orellana, M.; Gómez, H.; Córdova, R.; Dalchiele, E.; *Electrochim. Acta* **2001** *46* 4309.

6. Szabó, S.; Bakos, I.; *J. Electroanal. Chem.* **2000**, *492*, 103.

7. Szabó, S.; Bakos, I. In *Preparation of Catalysts VII. Studies in Surface Science and Catalysis*; Delmon, E. B.; Jacobs, P.A. et al. eds. **1998**, *118*, 269.

8. Zerbino, J. O.; Florit, M. I.; Maltz, A.; *Electrochim. Acta.* **1999**, *44*, 1973.

9. Fletcher, R.; Reeves, C. M.; *Computer J.* **1964**, *7*, 149.

10. Krishna, M. G.; Bhattacharrya, A. K.; *Solid. State Commun.* **2000**, *116*, 637.

11. Aspnes, D. E. In *Handbook of Optical Constants of Solids*; Palik, E. D. ed., Acad. Press: New York, ch. 5, p. 89.

12. Zerbino, J.; Castro Luna, A. M.; Zinola, C. F.; Méndez, E.; Martins, M. E.; *J. Electroanal. Chem.* **2002**, *521*, 168.

13. *CRC Handbook of Chem. and Phys.*, 73rd ed., CRC Press: D. R. Lide 1993.

14. Feinleib, J.; Scouler, W. J.; Ferretti, A.; *Phys. Rev.* **1968**, *165*, 765.

15. Gottesfeld, S.; Maia, G.; Floriano, J. B.; Tremiliosi Filho, G.; Ticianelli, E. A.; Gonzalez, E. R.; *J. Electrochem. Soc.* **1991**, *138*, 3219.

16. Horkans, J.; Cahan, B. D.; Yeager, E.; *Surf. Sci.* **1974**, *46*, 1.